

# Nanotopography-Promoted Formation of Axon Collateral Branches of Hippocampal Neurons

Jeongyeon Seo, Juan Kim, Sunghoon Joo, Ji Yu Choi, Kyungtae Kang,\* Woo Kyung Cho,\* and Insung S. Choi\*

**Axon collateral branches, as a key structural motif of neurons, allow neurons to integrate information from highly interconnected, divergent networks by establishing terminal boutons. Although physical cues are generally known to have a comprehensive range of effects on neuronal development, their involvement in axonal branching remains elusive. Herein, it is demonstrated that the nanopillar arrays significantly increase the number of axon collateral branches and also promote their growth. Immunostaining and biochemical analyses indicate that the physical interactions between the nanopillars and the neurons give rise to lateral filopodia at the axon shaft via cytoskeletal changes, leading to the formation of axonal branches. This report, demonstrates that nanotopography regulates axonal branching, and provides a guideline for the design of sophisticated neuron-based devices and scaffolds for neuro-engineering.**

Recent experimental data, found rather in a scattered fashion, unceasingly echoes that we should delve into the deterministic roles of nanostructure-derived physical cues<sup>[1]</sup> in neuronal development. Since the reports, in 2010, that neurite outgrowth and neurite elongation are accelerated on the nanometric substrates, such as anodized aluminum oxide (AAO)<sup>[2]</sup> and electrospun fibers,<sup>[3]</sup> compared with a flat slide, the validity of the 2D, flat surface as a neuron-culture platform has been controversial.<sup>[4,5]</sup> Not to mention the faithful recapitulation of the *in vivo* situations in an *in vitro* setting for legitimate neuron studies,<sup>[6]</sup> advances in the field would make it possible

to control and manipulate the developmental and morphological processes of neuronal and glial cells at one's will for certain purposes and applications.<sup>[7,8]</sup> Although nanotopography so far enables the chemical control over elementary but important facets of neuronal development, such as onset of neurite outgrowth and neurite-elongation rates,<sup>[2–17]</sup> it has been elusive to manipulate more sophisticated neuronal processes including formation of axon collateral branches. Axonal branches are imperative in the proper neural functions, because they allow neurons to integrate information by establishing the axon terminals, the indispensable part of neurons in the development of presynaptic differentiation.<sup>[18–20]</sup> In this paper, we

report that a nanostructure-based culture platform induces the formation of axon branches, which would further advance our controllability of neuronal development *in vitro*.

The culture platforms in this work were fabricated by replica-molding AAO nanostructures with hard poly(dimethylsiloxane) (*h*-PDMS) (Figure 1a). Briefly, after obtaining the nanoporous AAO substrates, composed of cylindrical pores, with a proper pitch ( $\approx 400$  nm)<sup>[2]</sup> by optimizing the anodization voltage/time and the type/concentration of electrolytes,<sup>[21–23]</sup> the replica-molding step was followed by transfer of the *h*-PDMS nanopillar (NP) array to a transparent glass slide<sup>[24]</sup> for easy culture and characterizations of neurons. We generated three NP arrays with different heights by varying the second-anodization time (5 min:  $240 \pm 8$  nm (NP-5), 10 min:  $280 \pm 5$  nm (NP-10), and 15 min:  $338 \pm 8$  nm (NP-15)). The characteristics of the NP arrays, such as density, width, hydrophilicity, and roughness, were studied (Figure S1, Supporting Information). The density and diameter of NPs were  $5.2\text{--}6.7$  NP  $\mu\text{m}^{-2}$  and  $105\text{--}113$  nm, respectively, and the NP substrates were highly hydrophobic (water contact angle:  $135\text{--}143^\circ$ ). Primary hippocampal neurons dissociated from embryonic day 18 (E18) Sprague Dawley rat hippocampi were cultured on the NP arrays after coating with poly-D-lysine (PDL), a positively charged neuro-adhesive polymer.<sup>[25]</sup>

Based on the previous reports on neuronal ability to distinguish the nanometer-scaled pitches of the culture substrates,<sup>[4]</sup> we investigated the prototypical nanotopography-effect of the NP arrays—accelerated neurite outgrowth, by measuring the longest-neurite length at 1 and 2 DIV (DIV: days *in vitro*) with the flat *h*-PDMS substrate as a control (Figure S2, Supporting

J. Seo, J. Kim, Dr. S. Joo, J. Y. Choi, Prof. I. S. Choi  
Department of Chemistry  
Center for Cell-Encapsulation Research  
KAIST

Daejeon 34141, South Korea  
E-mail: ischoi@kaist.ac.kr

Prof. K. Kang  
Department of Applied Chemistry  
Kyung Hee University  
Yongin, Gyeonggi 17104, South Korea  
E-mail: kkang@khu.ac.kr

Prof. W. K. Cho  
Department of Chemistry  
Chungnam National University  
Daejeon 34134, South Korea  
E-mail: wkcho@cnu.ac.kr

 The ORCID identification number(s) for the author(s) of this article can be found under <https://doi.org/10.1002/sml.201801763>.

DOI: 10.1002/sml.201801763

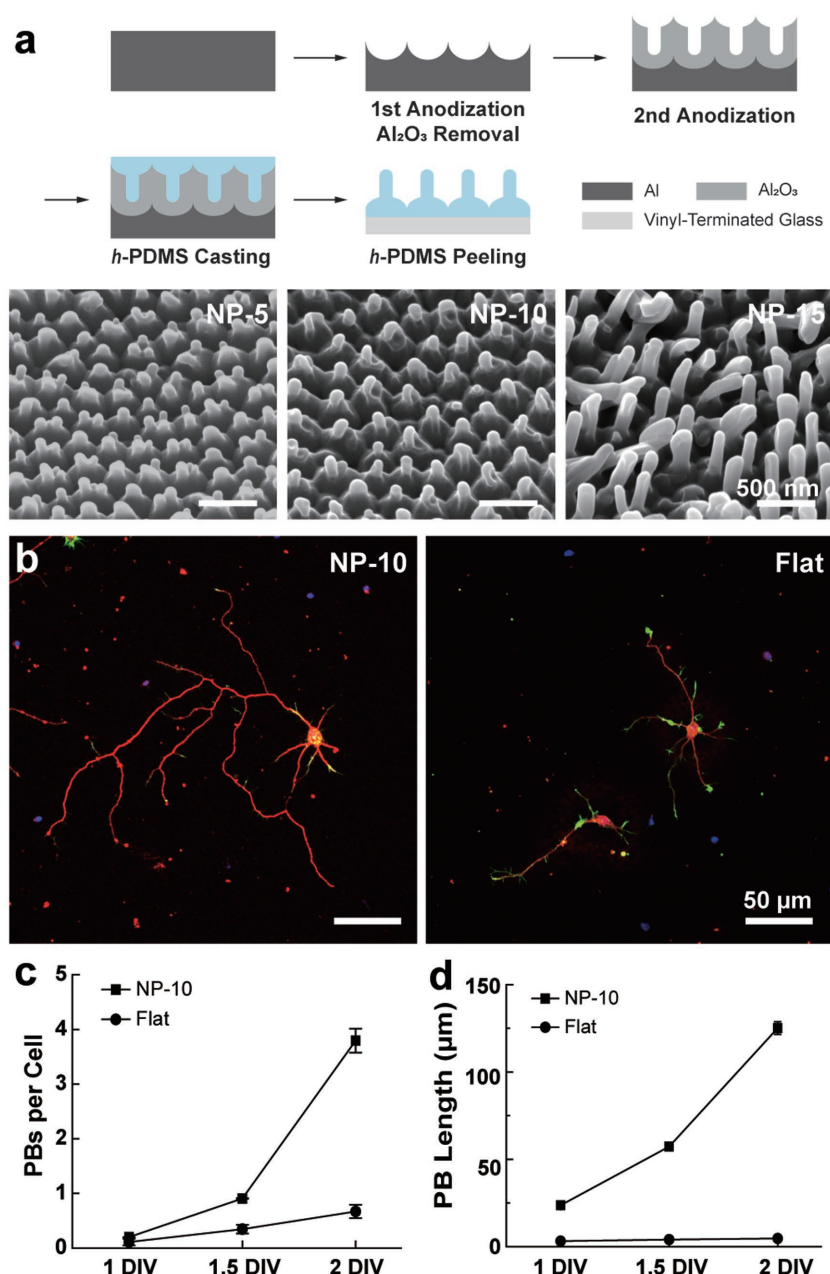


**Figure 1.** a) Schematic illustration for the fabrication of *h*-PDMS nanopillar arrays and field-emission scanning electron microscopy (FE-SEM) micrographs (tilt angle: 33°) of the nanopillar arrays. b) Confocal laser-scanning microscopy (CLSM) micrographs of the neurons on the NP-10 and flat substrates at 2 DIV. c) The averaged PB number (mean ± S.E.) per neuron on the NP-10 and flat substrates at 1, 1.5, and 2 DIV. d) The averaged PB length (mean ± S.E.) on the NP-10 and flat substrates at 1, 1.5, and 2 DIV.

Information). The analysis showed that the averaged longest-neurite length on NP-10 ( $208.0 \pm 9.7 \mu\text{m}$ ) was significantly greater than that on the flat control ( $71.6 \pm 7.7 \mu\text{m}$ ) at 2 DIV, and the neurite elongation was noticeably accelerated even at 1 DIV (NP-10:  $123.9 \pm 3.4 \mu\text{m}$ , control:  $31.5 \pm 2.0 \mu\text{m}$ ). Further analysis with NP-5 and NP-15 indicated that the nanopillar height did not noticeably affect the neurite outgrowth (Figure S3, Supporting Information), because the narrow interpillar distance ( $\approx 400 \text{ nm}$ ) in respect to the pillar diameter ( $\approx 100 \text{ nm}$ ) would

make the neurons interact mainly with the upper region of the nanopillars (Figure S4, Supporting Information),<sup>[2,26]</sup> while very thin neurite-like structures were found within the lower region of the nanopillars.<sup>[27]</sup> Based on these initial characterizations, NP-10 was selected for further, detailed studies, by considering that the NP-10 nanopillars were much more uniform without collapse compared with NP-5 and NP-15 ones (Figure 1a), and all the three substrates had the same nanotopographical effects on neurite outgrowth statistically (Figure S3, Supporting Information). The earlier-stage development of neurons on NP-10 was additionally characterized at 9, 15, and 21 h (Figure S5, Supporting Information).<sup>[6]</sup> At 9 h of culture, more than a half of the neurons on NP-10 developed to stages 2 and 3, while most of the neurons (>80%) were still at stage 1 for the control.<sup>[28]</sup> The accelerated development was more prominent at 21 h: more than 80% of the neurons reached stage 3 on NP-10, but only 3% of the neurons were at stage 3 on the control. In addition to the accelerated neurogenesis, NP-10 induced the early determination of a major neurite, reminiscent of our previous work.<sup>[6]</sup>

In addition to the prototypical effects of nanostructures on neuronal development, we surprisingly found that the hippocampal neurons on NP-10 greatly induced the formation of axon collateral branches (Figure 1b), which is essential for structural complexity and proper neural functions, such as learning, memory, sensory processing, and response.<sup>[29]</sup> Heretofore, there have been several reports that the formation of axonal branches is promoted by adjustment of mechanical tensions (e.g., substrate stiffness).<sup>[30–32]</sup> To quantitatively analyze the axonal branches, two indicators—primary branch (PB) and secondary branch (SB)—were used in this study (Figure S6, Supporting Information): PB was defined as the branch that sprouted directly from an axon, and SB as the one that sprouted from PB. At 1 DIV, the averaged PB number was less than unity for both NP-10 and the control (NP-10:  $0.2 \pm 0.01$ , control:  $0.1 \pm 0.1$ ), and the value increased slightly more at 1.5 DIV (NP-10:  $0.9 \pm 0.1$ , control:  $0.4 \pm 0.1$ ) (Figure 1c). However, explosive PB formation was observed at 2 DIV only in the case of NP-10: at 2 DIV, the PB number increased sharply to about 4 ( $3.8 \pm 0.2$ ), while insignificant linear increase occurred for the control ( $0.7 \pm 0.1$ ). The enhanced PB elongation was also observed exclusively on NP-10 (Figure 1d): the averaged PB length on NP-10 was  $23.7 \pm 0.1$ ,  $57.3 \pm 1.3$ , and  $125.1 \pm 3.6 \mu\text{m}$  at 1, 1.5, and 2 DIV, respectively, but the value was less than  $5 \mu\text{m}$  for the control

( $3.1 \pm 0.1 \mu\text{m}$  at 1 DIV,  $4.0 \pm 0.2 \mu\text{m}$  at 1.5 DIV, and  $4.7 \pm 0.1 \mu\text{m}$  at 2 DIV). Additional hippocampal branches are developed in the interstitial mode where axon branches form behind the growth cone of the axon terminal, not in a bifurcation mode where axon branches are formed by splitting of the growth cone.<sup>[20,28,29,33]</sup> Therefore, the observation that PB elongation length of  $101.4 \mu\text{m}$  between 1 and 2 DIV on NP-10 was of the same order as the major-neurite elongation for the first 1-DIV period ( $123.9 \mu\text{m}$ ) implied that the development of axonal branches and neurites was promoted via similar mechanisms by the NP-10 topography. No, or little if any, PB elongation on the flat control additionally indicated that the NP-10 nanopillars specifically accelerated the axon development.<sup>[19]</sup> NP-10 also induced the increased formation of higher-order branches (Figure S7, Supporting Information). The ratio of the number of SBs to that of PBs was 0.24 at 2 DIV for NP-10, but the ratio was about 0.1 for the other cases.

Biological studies show that axonal branching is initiated by the reorganization of actin and microtubules at the localized regions of an axon, which is much similar to what happens at the growth cone during axonal outgrowth.<sup>[34–37]</sup> Chemical cues to axon-branch formation have been indentified;<sup>[38,39]</sup> for example, netrin-1,<sup>[40,41]</sup> Ephrin A,<sup>[42,43]</sup> nerve growth factors,<sup>[44,45]</sup> and brain-derived neurotrophic factors<sup>[46]</sup> regulate the reorganization and movement of cytoskeleton to promote the formation of axonal branches. Therefore, we first counted the number of lateral filopodia to investigate the effects of NP-10 on cytoskeletal dynamics at the axon shaft (Figure 2a). Because the developmental rates of neurons were different for NP-10

and the control, the analysis was performed only with the stage-3 neurons, which already determined their axons, at 1 DIV for NP-10 and at 2 DIV for the control. The analysis indicated that lateral filopodia were present, on average, every  $5 \mu\text{m}$  of the axon shaft for NP-10, but less than one filopodium was observed per  $10 \mu\text{m}$  of the axon shaft in the case of the control (Figure 2b). The magnified FE-SEM images showed that the lateral filopodia interacted intimately with the nanopillars, indicating that the enhanced formation of lateral filopodia was induced by physical interactions (Figure 2c). The results clearly confirmed that the NP structures gave rise to lateral filopodia that are potential sites for axonal branching. This observation was also consistent with the previous reports that mammalian cells on the microposts and nanowires formed focal adhesions over the discontinuous contact points,<sup>[47,48]</sup> inducing the spatial localization of actin-related protein complexes and the local condensation of actin.<sup>[49,50]</sup> This local contact of axons on upper region of discontinuous topography could explain the formation of neuronal network and axon branching on the microstructure with lower roughness in line with our results.<sup>[27,51–53]</sup> Taken all together, we believe that the NP-10 nanopillar arrays triggered the axonal branching by forming discontinuous adhesion points with axons and bringing about actin condensation.

We also treated the neurons with three biochemical inhibitors—cytochalasin D, nocodazole, and blebbistatin—that interfere with cytoskeletal dynamics in different fashions (Figure 3). The neurons on NP-10 were treated with each inhibitor at 18 h after plating (i.e., after axon formation) and characterized by CLSM at 2 DIV (Figure 3a). One of the salient inhibition effects against formation of axon branches was found in the treatment of cytochalasin D, actin-polymerization inhibitor, which abolished the formation of both lateral filopodia and axon branches (Figure 3b). Therefore, this result further supported the hypothesis that the formation of lateral filopodia is a crucial prerequisite toward the formation of axonal branches in our system. We additionally found that cytoskeletal dynamics at the axon shaft was orchestrated for the branch formation on NP-10, because the inhibition of microtubule polymerization, by nocodazole, did not form the axon lateral branches, although the formation of lateral filopodia was not affected. Blebbistatin, a nonmuscle myosin II inhibitor, decreased the number of lateral filopodia to some extent and, consequently, the formation of axon branches. Taken all together, it could be concluded that the NP-10 nanostructures provided physical cues to the controlled axon-branch formation by directly changing the cytoskeleton structures and their dynamics at the axon shaft, similarly to what it does to the ones at the tip of neurites.<sup>[33,38,54]</sup>

In summary, we demonstrated that the nanopillar array (pitch:  $400 \text{ nm}$ ) significantly promoted the formation of axon collateral branches de novo<sup>[20]</sup> by changing the cytoskeleton dynamics at the axon shaft. A consensus

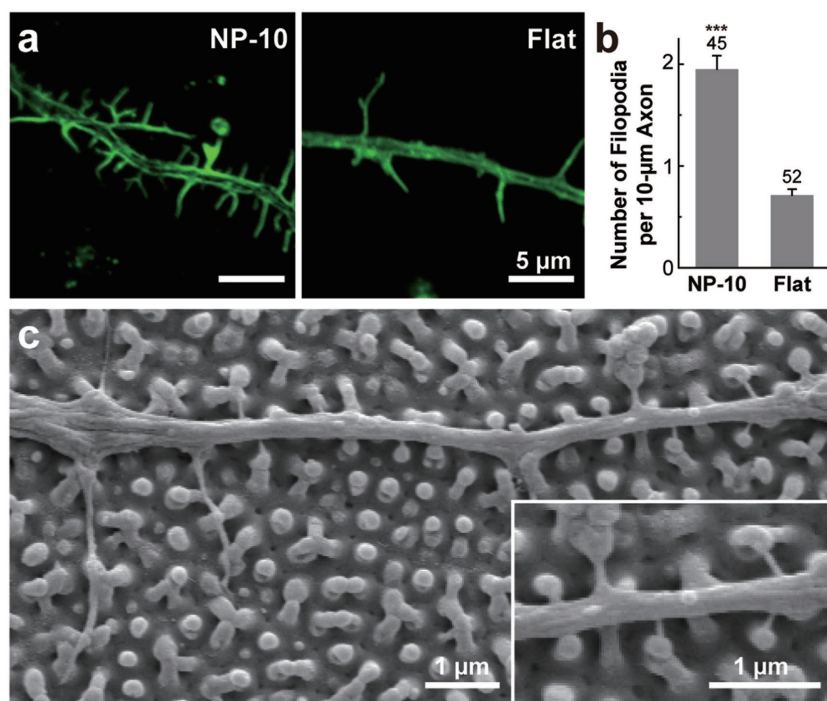


**Figure 2.** Increased formation of lateral filopodia from an axon shaft on NP-10. a) CLSM micrographs of the axons on the NP-10 and flat substrates. Neurons were observed after staining of F-actin (green). b) The averaged number (mean  $\pm$  S.E.) of filopodia per  $10 \mu\text{m}$  axonal segment on the NP-10 and flat substrates. A two-tailed unpaired Student's *t*-test ( $***p < 0.001$ ) was used to compare two samples. c) FE-SEM micrographs of the neurite on NP-10 at 1 DIV.



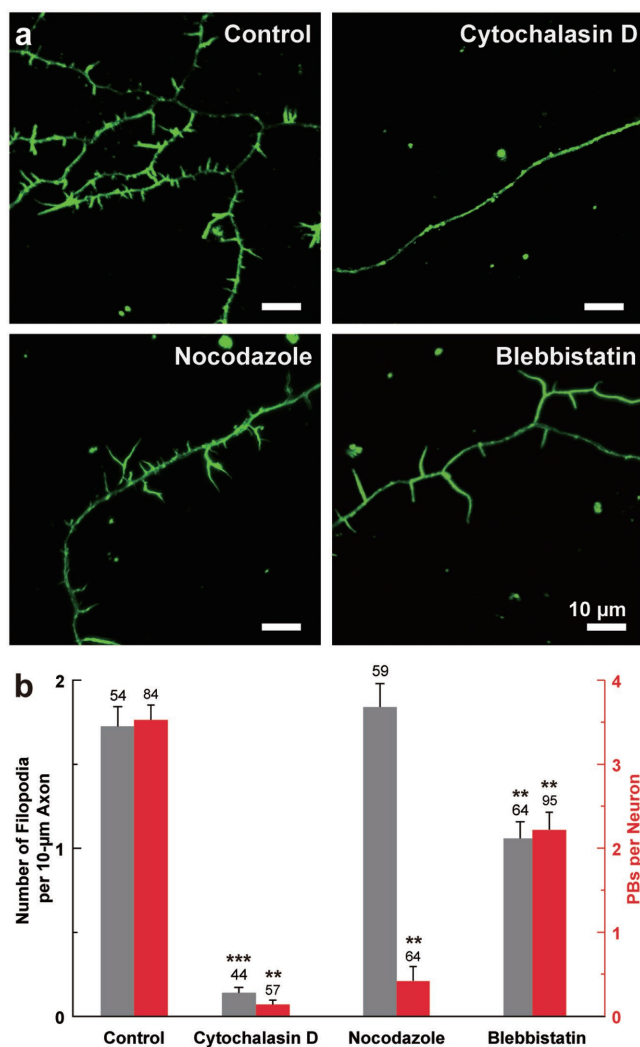


**Figure 3.** Effects of the biochemical inhibitors on the formation of axonal branches. a) CLSM micrographs of the neurons on NP-10 after being treated with each inhibitor. Neurons were observed by staining of F-actin (green) at 2 DIV. b) Averaged number (mean  $\pm$  S.E.) of filopodia per 10  $\mu$ m axonal segment and average PB number (mean  $\pm$  S.E.) per neuron on NP-10 after treatment with each inhibitor. The comparison with the control group was performed by one-way ANOVA at a significant level of 95%, followed by Bonferroni's multiple comparison test ( $^{**}p < 0.01$ ,  $^{***}p < 0.001$ ).

has arisen, in the communities of neurochemistry and related fields, that nanotopography, as one of the physical cues, accelerates neurite outgrowth, guides axon elongation, and induces neuron development with fewer neurites in vitro. Fundamental studies have been executed to identify the genes and proteins in charge of this unforeseen phenomenon and elucidate the underlying mechanisms, along with studies on its in vivo relevance. The nanotopography-derived in vitro controllability also has been applied to neuroregenerative scaffolds<sup>[55–61]</sup> including treatment of spinal cord injury. The current work affirmatively indicates that the roles of nanometric structures in the neuronal development are to explore further, and our understanding is limited. Nonetheless, its result, enhanced formation of axon collateral branches by nanotopography, adds an

advanced toolbox to the in vitro manipulation of developmental behavior of neurons.

## Experimental Section

**Neuron Culture:** Primary hippocampal neurons from the hippocampi of E18 Sprague-Dawley rat pups were cultured in serum-free conditions. Hippocampi were dissected and dissociated to single cells in Hank's Balanced salt solution, centrifuged at 1000 rpm, and resuspended in Neurobasal Medium with B-27 supplement, GlutaMAX, L-glutamic acid, and 1% penicillin-streptomycin. Dissociated neurons were seeded on NP-10 at a density of 50 cells  $\text{mm}^{-2}$  and cultured at 37  $^{\circ}\text{C}$  in a humidified atmosphere of 5%  $\text{CO}_2$ . This study was approved by the IACUC (Institutional Animal Care and Use Committee) of KAIST.

## Supporting Information

Supporting Information is available from the Wiley Online Library or from the author.

## Acknowledgements

J.S. and J.K. contributed equally to this work. This work was supported by the National Research Foundation of Korea (NRF) grant funded by the Ministry of Science, ICT & Future Planning (MSIP) (2012R1A3A2026403 to I.S.C., 2016R1A1A1A05921718 to W.K.C., and 2016R1C1B2011414 to K.K.).

## Conflict of Interest

The authors declare no conflict of interest.

## Keywords

axon collateral branches, lateral filopodia, nanopillar arrays, nanostructures, neurochemistry

Received: May 8, 2018

Revised: June 23, 2018

Published online:

- [1] P. Weiss, *J. Exp. Zool.* **1934**, 68, 393.
- [2] W. K. Cho, K. Kang, G. Kang, M. J. Jang, Y. Nam, I. S. Choi, *Angew. Chem., Int. Ed.* **2010**, 49, 10114.
- [3] C. C. Gertz, M. K. Leach, L. K. Birrell, D. C. Martin, E. L. Feldman, J. M. Corey, *Dev. Neurobiol.* **2010**, 70, 589.
- [4] M.-H. Kim, M. Park, K. Kang, I. S. Choi, *Biomater. Sci.* **2014**, 2, 148.
- [5] C. Simitzi, A. Ranella, E. Stratakis, *Acta Biomater.* **2017**, 51, 21.
- [6] K. Kang, Y.-S. Park, M. Park, M. J. Jang, S.-M. Kim, J. Lee, J. Y. Choi, D. H. Jung, Y.-T. Chang, M.-H. Yoon, J. Lee, H. Cho, S.-P. Hong, S. H. Yang, S. H. Jung, S.-B. Ko, I. S. Choi, *Nano Lett.* **2016**, 16, 675.
- [7] M. Marcus, K. Baranes, M. Park, I. S. Choi, K. Kang, O. Shefi, *Adv. Healthcare Mater.* **2017**, 6, 1700267.
- [8] H. K. Kim, E. Kim, H. Jang, Y.-K. Kim, K. Kang, *ChemNanoMat* **2017**, 3, 278.
- [9] P. G elle, M.-T. Perez, C. N. Prinz, *Biomaterials* **2013**, 34, 875.

- [10] K. Kang, S. Y. Yoon, S.-E. Choi, M.-H. Kim, M. Park, Y. Nam, J. S. Lee, I. S. Choi, *Angew. Chem., Int. Ed.* **2014**, *53*, 6075.
- [11] K. Kang, S.-E. Choi, H. S. Jang, W. K. Cho, Y. Nam, I. S. Choi, J. S. Lee, *Angew. Chem., Int. Ed.* **2012**, *51*, 2855.
- [12] S.-M. Kim, S. Lee, D. Kim, D.-H. Kang, K. Yang, S.-W. Cho, J. S. Lee, I. S. Choi, K. Kang, M.-H. Yoon, *Nano Res.* **2018**, *11*, 2532.
- [13] J. Xie, W. Liu, M. R. MacEwan, P. C. Bridgman, Y. Xia, *ACS Nano* **2014**, *8*, 1878.
- [14] G. Bugnicourt, J. Brocard, A. Nicolas, C. Villard, *Langmuir* **2014**, *30*, 4441.
- [15] K. Baranes, M. Shevach, O. Shefi, T. Dvir, *Nano Lett.* **2016**, *16*, 2916.
- [16] K.-J. Jang, M. S. Kim, D. Feltrin, N. L. Jeon, K.-Y. Suh, O. Pertz, *PLoS ONE* **2010**, *5*, e15966.
- [17] C. Schulte, M. Ripamonti, E. Maffioli, M. A. Cappelluti, S. Nonnis, L. Puricelli, J. Lamanna, C. Piazzoni, A. Podestà, C. Lenardi, G. Tedeschi, A. Malgaroli, P. Milani, *Front. Cell Neurosci.* **2016**, *10*, 267.
- [18] N. Arimura, K. Kaibuchi, *Nat. Rev. Neurosci.* **2007**, *8*, 194.
- [19] T. L. Lewis Jr., J. Courchet, F. Polleux, *J. Cell Biol.* **2013**, *202*, 837.
- [20] D. D. M. O'Leary, T. Terashima, *Neuroendocrinology* **1988**, *1*, 901.
- [21] W. Lee, S.-J. Park, *Chem. Rev.* **2014**, *114*, 7487.
- [22] O. Jessensky, F. Müller, U. Gösele, *Appl. Phys. Lett.* **1998**, *72*, 1173.
- [23] A. P. Li, F. Müller, A. Birner, K. Nielsch, U. Gösele, *J. Appl. Phys.* **1998**, *84*, 6023.
- [24] K.-B. Lee, Y. H. Jung, Z.-W. Lee, S. Kim, I. S. Choi, *Biomaterials* **2007**, *28*, 5594.
- [25] P. C. Letourneau, *Dev. Biol.* **1975**, *44*, 77.
- [26] L. Hanson, Z. C. Lin, C. Xie, Y. Cui, B. Cui, *Nano Lett.* **2012**, *12*, 5815.
- [27] C. Simitzi, P. Efstathopoulos, A. Kourgiantaki, A. Ranella, I. Charalampopoulos, C. Fotakis, I. Athanassakis, E. Stratakis, A. Gravanis, *Biomaterials* **2015**, *67*, 115.
- [28] C. G. Dotti, C. A. Sullivan, G. A. Banker, *J. Neurosci.* **1988**, *8*, 1454.
- [29] L. Armijo-Weingart, G. Gallo, *Mol. Cell. Neurosci.* **2017**, *84*, 36.
- [30] A. Kostic, J. Sap, M. P. Sheetz, *J. Cell Sci.* **2007**, *120*, 3895.
- [31] L. A. Fianagan, Y.-E. Ju, B. Marg, M. Osterfield, P. A. Janmey, *NeuroReport* **2002**, *13*, 2411.
- [32] D. E. Koser, A. J. Thompson, S. K. Foster, A. Dwivedy, E. K. Pillai, G. K. Sheridan, H. Svoboda, M. Viana, L. da F. Costa, J. Guck, C. E. Holt, K. Franze, *Nat. Neurosci.* **2016**, *19*, 1592.
- [33] W. Yu, F. J. Ahmad, P. W. Baas, *J. Neurosci.* **1994**, *14*, 5872.
- [34] L. A. Lowery, D. Van Vactor, *Nat. Rev. Mol. Cell Biol.* **2009**, *10*, 332.
- [35] E. A. Vitriol, J. Q. Zheng, *Neuroendocrinology* **2012**, *73*, 1068.
- [36] E. W. Dent, F. B. Gertler, *Neuroendocrinology* **2003**, *40*, 209.
- [37] K. Kalil, G. Szebenyi, *J. Neurobiol.* **2000**, *44*, 145.
- [38] K. Kalil, E. W. Dent, *Nat. Rev. Neurosci.* **2014**, *15*, 7.
- [39] G. Gallo, *Dev. Neurobiol.* **2011**, *71*, 201.
- [40] C. Manitt, A. M. Nikolakopoulou, D. R. Almario, S. A. Nguyen, S. Cohen-Cory, *J. Neurosci.* **2009**, *29*, 11065.
- [41] E. W. Dent, A. M. Barnes, F. Tang, K. Kalil, *J. Neurosci.* **2004**, *24*, 3002.
- [42] P. A. Yates, A. L. Roskies, T. McLaughlin, D. D. O'Leary, *J. Neurosci.* **2001**, *21*, 8548.
- [43] I. Galimberti, E. Bednarek, F. Donato, P. Caroni, *Neuroendocrinology* **2010**, *65*, 627.
- [44] N. O. Glebova, *J. Neurosci.* **2004**, *24*, 743.
- [45] S. I. Lentz, C. M. Knudson, S. J. Korsmeyer, W. D. Snider, *J. Neurosci.* **1999**, *19*, 1038.
- [46] S. Cohen-Cory, *J. Neurosci.* **1999**, *19*, 9996.
- [47] M. Nikkha, F. Edalat, S. Manoucheri, A. Khademhosseini, *Biomaterials* **2012**, *33*, 5230.
- [48] C. Prinz, W. Hällström, T. Mårtensson, L. Samuelson, L. Montelius, M. Kanje, *Nanotechnology* **2008**, *19*, 345101.
- [49] T. Iskratsch, H. Wolfenson, M. P. Sheetz, *Nat. Rev. Mol. Cell Biol.* **2014**, *15*, 825.
- [50] F. M. Watt, W. T. S. Huck, *Nat. Rev. Mol. Cell Biol.* **2013**, *14*, 467.
- [51] E. L. Papadopoulou, A. Samara, M. Barberoglou, A. Manousaki, S. N. Pagakis, E. Anastasiadou, C. Fotakis, E. Stratakis, *Tissue Eng., Part C* **2009**, *16*, 479.
- [52] L. Micholt, A. Gärtner, D. Prodanov, D. Bradken, C. G. Dotti, C. Bartic, *PLoS ONE* **2013**, *8*, e66170.
- [53] K. Baranes, D. Kollmar, N. Chejanovsky, A. Sharoni, O. Shefi, *J. Mol. Histol.* **2012**, *43*, 437.
- [54] E. W. Dent, F. Tang, K. Kalil, *Neuroscientist* **2003**, *9*, 343.
- [55] N. J. Schaub, C. D. Johnson, B. Cooper, R. J. Gilbert, *J. Neurotrauma* **2016**, *33*, 1405.
- [56] A. P. Weightman, M. R. Pickard, Y. Yang, D. M. Chari, *Biomaterials* **2014**, *35*, 3756.
- [57] M. Antman-Passig, O. Shefi, *Nano Lett.* **2016**, *16*, 2567.
- [58] M. Antman-Passig, S. Levy, C. Gartenberg, H. Schori, O. Shefi, *Tissue Eng., Part A* **2017**, *23*, 403.
- [59] J. M. Corey, C. C. Gertz, B.-S. Wang, L. K. Birrell, S. L. Johnson, D. C. Martin, E. L. Feldman, *Acta Biomater.* **2008**, *4*, 863.
- [60] E. K. Purcell, Y. Naim, A. Yang, M. K. Leach, J. M. Velkey, R. K. Duncan, J. M. Corey, *Biomacromolecules* **2012**, *13*, 3427.
- [61] S. Hackelberg, S. J. Tuck, L. He, A. Rastogi, C. White, L. Liu, D. M. Prieskorn, R. J. Miller, C. Chan, B. R. Loomis, J. M. Corey, J. M. Miller, R. K. Duncan, *PLoS ONE* **2017**, *12*, e0180427.